

# Nucleophilic Dearomatization of N-Heteroaromatics Enabled by Lewis Acids and Copper Catalysis

Xingchen Yan,<sup>†</sup> Luo Ge,<sup>†</sup> Marta Castiñeira Reis, and Syuzanna R. Harutyunyan\*

Cite This: <https://dx.doi.org/10.1021/jacs.0c09974>

Read Online

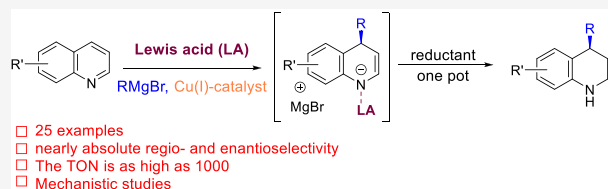
ACCESS |

Metrics & More

Article Recommendations

Supporting Information

**ABSTRACT:** Dearomative functionalization of heteroaromatics, a readily available chemical feedstock, is one of the most straightforward approaches for the synthesis of three-dimensional, chiral heterocyclic systems, important synthetic building blocks for both synthetic chemistry and drug discovery. Despite significant efforts, direct nucleophilic additions to heteroaromatics have remained challenging because of the low reactivity of aromatic substrates associated with the loss of aromaticity, as well the regio- and stereoselectivities of the reaction. Here we present a catalytic system that leads to unprecedented, high-yielding dearomative C-4 functionalization of quinolines with organometallics with nearly absolute regio- and stereoselectivities and with a catalyst turnover number (TON) as high as 1000. The synergistic action of the chiral copper catalyst, Lewis acid, and Grignard reagents allows us to overcome the energetic barrier of the dearomatization process and leads to chiral products with selectivities reaching 99% in most cases. Molecular modeling provides important insights into the speciation and the origin of the regio- and enantioselectivity of the catalytic process. The results reveal that the role of the Lewis acid is not only to activate the substrate toward a potential nucleophilic addition but also to subtly control the regiochemistry by preventing the C-2 addition from happening.



- 25 examples
- nearly absolute regio- and enantioselectivity
- The TON is as high as 1000
- Mechanistic studies

## INTRODUCTION

Optically active, nitrogen-containing heterocycles are important structural constructs found in a myriad of natural products, biologically active molecules, and pharmaceutically active ingredients.<sup>1,2</sup> It has been shown that complex three-dimensional chiral molecules are more likely to show useful bioactive properties than achiral, flat aromatic compounds, because of improved interactions with the target proteins.<sup>3</sup> The chiral hydroquinoline motif is a particularly relevant heterocyclic system, as it is present in many natural and unnatural compounds with interesting biological properties, and therefore, their synthesis is of great interest for synthetic chemistry, the agrochemical industry, and for drug discovery (Scheme 1a).<sup>1,2</sup> As a result, both noncatalytic and catalytic strategies have been described for the synthesis of chiral hydroquinoline derivatives.<sup>2</sup>

Nucleophilic dearomative addition to nitrogen-containing heteroaromatics is arguably one of the most straightforward approaches to synthesize chiral azaheterocycles.<sup>4</sup> However, direct nucleophilic addition to heteroaromatic compounds is challenging: their reactivity is low because the addition is only possible at the cost of loss of aromaticity.<sup>5</sup> The most common strategy to circumvent this reactivity issue consists of activating the heteroaromatic ring with a reactive electrophile to form a heteroarenium salt, followed by a nucleophilic attack. This approach has also been applied to quinolines.<sup>5,6</sup> In nucleophilic dearomative additions to quinolines and quinolinium salts, apart from reactivity issues, enantioselectivity and regiocontrol are additional hurdles, since there are two electrophilic

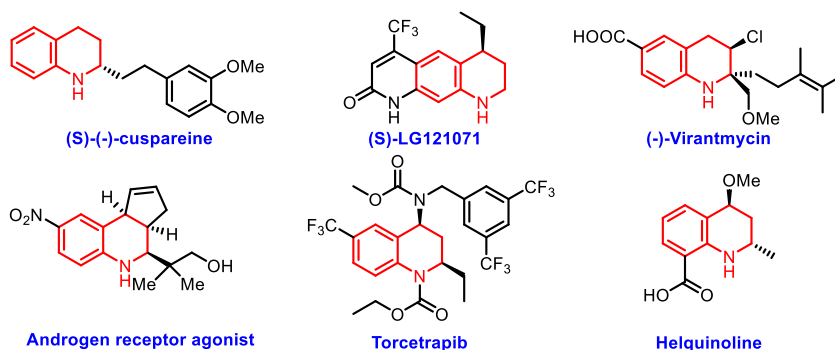
positions that can undergo nucleophilic attack, namely, the C-2 and C-4 position (Scheme 1b).<sup>6a–g</sup> Interestingly, analysis of the literature reveals not only that all successful strategies for nucleophilic additions to quinoline derivatives require quinolinium salts but also that the overwhelming majority of both racemic and enantioselective methods feature a nucleophilic attack at the C-2 position.<sup>6g,h,7</sup> The only reported example of direct asymmetric addition to quinolines to date takes advantage of the high reactivity of organolithium reagents but provides the C-2-addition products with a modest enantioselectivity (58–79%) while requiring a large (20–100 mol %) loading of a chiral ligand (Scheme 1b).<sup>6h,7</sup> Moreover, there are no precedents of catalytic asymmetric additions to the C-4 position of both quinolines or quinolinium salts. Only diastereoselective C-4 addition to quinolines has been reported, but these methodologies require chiral auxiliaries or preformed chiral nucleophiles and suffer from severe scope limitation.<sup>8</sup>

Realizing that the N–C-2–C-4 fragment of quinoline can be viewed as a masked  $\alpha,\beta$ -unsaturated conjugated imine moiety, we envisioned a possible strategy for the enantioselective

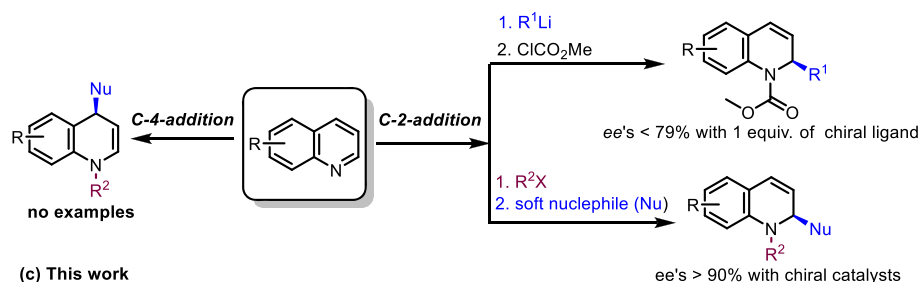
Received: September 17, 2020

**Scheme 1. Importance of Chiral Tetrahydroquinoline Derivatives with Methods for Their Asymmetric Synthesis and Current Work:** (a) Natural Products and Drugs Incorporating Chiral Tetrahydroquinolines; (b) State of the Art in Nucleophilic Additions to Quinoline and Quinolinium Salts; (c) Main Idea Behind the Current Work

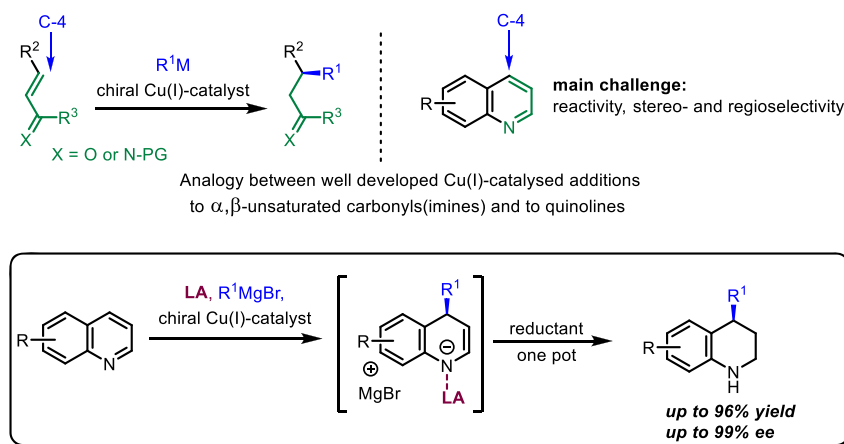
(a) Natural products and drugs incorporating chiral tetrahydroquinolines



(b) Nucleophilic additions to quinoline and quinolinium salts: state of the art



(c) This work



dearomative C-4 functionalization of quinolines (Scheme 1c). Rather than relying on premade quinolinium salts, a suitable Lewis acid (LA) could act as a transient activator of the quinoline ring toward nucleophilic addition.<sup>9</sup> A catalyst can then be used to direct the nucleophile to the required C-4 position with a high level of enantiodiscrimination, as the C-3–C-4 double bond should be susceptible to copper-catalyzed conjugate addition of organometallics, a classic method for asymmetric conjugate additions to  $\alpha,\beta$ -unsaturated carbonyl compounds.<sup>10</sup> Thus, it should be possible to use copper(I)-based catalysts to direct the addition of organometallics toward the C-4 position. We anticipated that the unique reactivity provided by the combination of LA, copper(I) catalysis, and Grignard reagents previously demonstrated by our group<sup>11</sup> would be able to overcome the energetic barrier of nucleophilic dearomative addition to quinolines.

Herein, we present the first catalytic system that allows highly selective catalytic enantioselective nucleophilic dearomatization of quinolines with organometallics (Scheme 1c). The synergistic combination of LA, chiral copper(I) catalyst, and Grignard reagents allows access to the C-4-addition products with nearly absolute regio- and stereocontrol. Remarkably, the amount of chiral copper catalyst can be reduced to 0.1 mol % in a preparative-scale reaction, representing the highest turnover number (TON) reported among any enantioselective reactions involving Grignard reagents. Comprehensive speciation and conformational analysis using molecular modeling provides insights into the role of the LA and the origin of the regio- and stereoselectivity.

## RESULTS AND DISCUSSION

Our investigation of the enantioselective dearomatization of quinolines began with the model reaction of quinoline 1a with

Table 1. Development of the Catalytic System for Dearomative C-4-Selective Functionalization of Quinoline<sup>a</sup>

entry	L	Cu(I)	LA	solvent	1a:2a:3a <sup>b</sup>	ee (2a) [%] <sup>c</sup>	ee (3a) [%] <sup>c</sup>
1 <sup>d</sup>				CH <sub>2</sub> Cl <sub>2</sub>	100:0:0		
2			Me <sub>3</sub> SiOTf	CH <sub>2</sub> Cl <sub>2</sub>	1:93:6		
3	L1	CuBr·SMe <sub>2</sub>		CH <sub>2</sub> Cl <sub>2</sub>	100:0:0		
4	L1	CuBr·SMe <sub>2</sub>	Me <sub>3</sub> SiOTf	CH <sub>2</sub> Cl <sub>2</sub>	3:79:18	7	77
5	L2	CuBr·SMe <sub>2</sub>	Me <sub>3</sub> SiOTf	CH <sub>2</sub> Cl <sub>2</sub>	0:87:13	rac	rac
6	L3	CuBr·SMe <sub>2</sub>	Me <sub>3</sub> SiOTf	CH <sub>2</sub> Cl <sub>2</sub>	0:81:19	rac	rac
7	L4	CuBr·SMe <sub>2</sub>	Me <sub>3</sub> SiOTf	CH <sub>2</sub> Cl <sub>2</sub>	0:88:12	7	45
8	L1	CuTc	Me <sub>3</sub> SiOTf	CH <sub>2</sub> Cl <sub>2</sub>	0:67:33	4	83
9	L1	CuTc	Et <sub>3</sub> SiOTf	CH <sub>2</sub> Cl <sub>2</sub>	36:19:45	6	32
10	L1	CuTc	<i>t</i> -BuMe <sub>2</sub> SiOTf	CH <sub>2</sub> Cl <sub>2</sub>	85:2:13		68
11	L1	CuTc	<i>i</i> -Pr <sub>3</sub> SiOTf	CH <sub>2</sub> Cl <sub>2</sub>	87:9:4		
12	L1	CuTc	<i>t</i> -BuPh <sub>2</sub> SiOTf	CH <sub>2</sub> Cl <sub>2</sub>	78:2:20		80
13 <sup>e</sup>			BF <sub>3</sub> ·Et <sub>2</sub> O	CH <sub>2</sub> Cl <sub>2</sub>	80:14:6		
14 <sup>e,f,g</sup>	L1	CuTc	BF <sub>3</sub> ·Et <sub>2</sub> O	CH <sub>2</sub> Cl <sub>2</sub>	1:0:99		>99
15 <sup>e</sup>	L4	CuTc	BF <sub>3</sub> ·Et <sub>2</sub> O	CH <sub>2</sub> Cl <sub>2</sub>	26:5:69		88
16 <sup>e</sup>	L1	CuTc	BF <sub>3</sub> ·Et <sub>2</sub> O	THF	12:81:7		42
17 <sup>e</sup>	L1	CuTc	BF <sub>3</sub> ·Et <sub>2</sub> O	2-Me-THF	1:0:99		>99
18 <sup>e,h</sup>	L1	CuTc	BF <sub>3</sub> ·Et <sub>2</sub> O	<i>t</i> -BuOMe	2:0:98		>99
19 <sup>e,h</sup>	L1	CuTc	BF <sub>3</sub> ·Et <sub>2</sub> O	toluene	1:0:99		>99
20 <sup>e,h</sup>	L1	CuTc	BF <sub>3</sub> ·Et <sub>2</sub> O	Et <sub>2</sub> O	2:0:98		>99

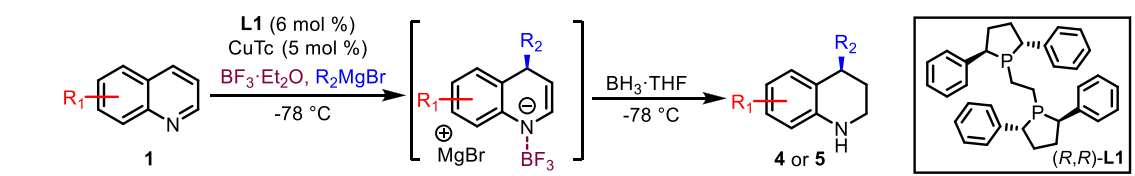
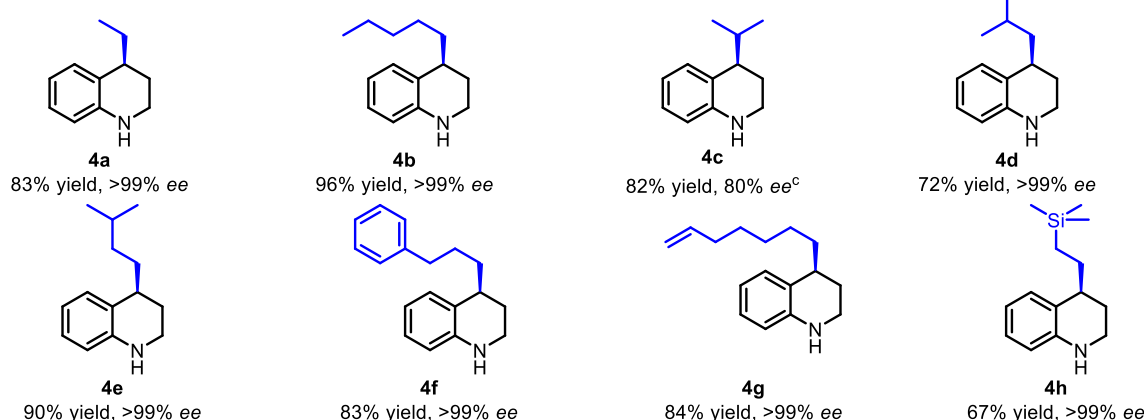
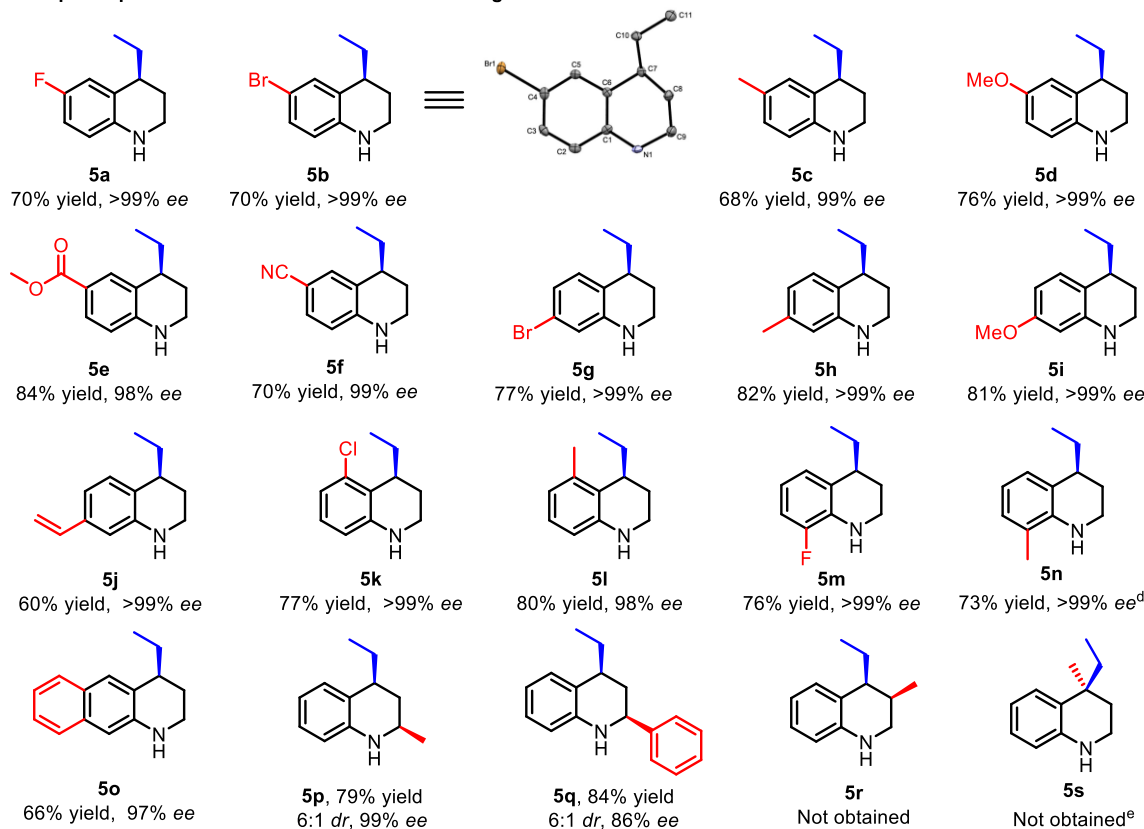
<sup>a</sup>Reaction conditions: 0.1 M **1a**, Cu(I) (5 mol %), L (6 mol %), LA (2 equiv), EtMgBr (2 equiv) at  $-78^{\circ}\text{C}$  for 16 h, and then ClCOMe (5 equiv) at RT for 2 h. <sup>b</sup>The ratio was determined by  $^1\text{H}$  NMR of reaction crude. <sup>c</sup>Enantiomeric excess was determined by HPLC on a chiral stationary phase. <sup>d</sup>In this case the reaction was quenched directly without trapping with ClCOMe. <sup>e</sup>In this case THF (4 mL) was added after addition of ClCOMe: when using BF<sub>3</sub>·Et<sub>2</sub>O trapping was only successful in THF. <sup>f</sup>A 58% isolated yield of **3a** and a complex mixture of byproducts was obtained. <sup>g</sup>Similar results were obtained when using CuBr·SMe<sub>2</sub> instead of CuTc (see the Supporting Information). <sup>h</sup>In this case 3 equiv of LA and 3 equiv of EtMgBr were used.

EtMgBr in CH<sub>2</sub>Cl<sub>2</sub> at  $-78^{\circ}\text{C}$  (Table 1) quenched with acetyl chloride upon reaction completion. The two anticipated regioisomeric products under these reaction conditions are products **2a** and **3a** resulting from nucleophilic attack of EtMgBr at either the C-2 or C-4 position, respectively, but neither was observed in the absence of any metal catalyst nor LA (Table 1, entry 1). To boost the reactivity of quinoline **1a** we added the highly reactive LA Me<sub>3</sub>SiOTf, which resulted in a significant reaction rate acceleration and nearly full conversion of the substrate **1a**. Analysis of the reaction crude revealed that the major product of the reaction derives from the nucleophilic attack at the C-2 position (Table 1, entry 2). Anticipating that Cu(I) salt may recognize the  $\alpha,\beta$ -unsaturated conjugated imine motif in the quinoline molecule, we also carried out the addition of EtMgBr in the presence of Cu(I) salt and Cu(I) complex with chiral ligand **L1**, but no conversion to either product **2a** or **3a** was observed (Table 1, entry 3). Combining the chiral copper catalyst system **L1**/Cu(I) with Me<sub>3</sub>SiOTf resulted, similarly as when adding the LA alone, in an immense acceleration of the addition reaction, but now with improved

selectivity toward the C-4-addition product, providing products **2a** and **3a** in a ratio of 79:18 (Table 1, entry 4).

Although still the minor product, the chiral C-4-addition product **3a** was obtained with 77% enantiomeric excess (ee), while in contrast, the C-2-addition product **2a** was obtained with only 7% ee. This result is crucial, since it indicates that the C-4 addition is mainly due to the catalytic reaction, while the C-2 addition is mainly produced by the noncatalyzed background reaction initiated by Me<sub>3</sub>SiOTf. This gave us confidence that further optimization of the catalyst and/or reaction conditions toward the catalytic C-4-addition pathway could lead to improved enantio- and regioselectivity. Bearing this in mind, we kicked off the optimization process by exploring the reactivity of several chiral ligands, **L2**–**L4**, in the presence of Me<sub>3</sub>SiOTf (Table 1, entries 5–7). These reactions afforded mainly the C-2-addition product **2a** as well as decreased enantioselectivity, leading us to conclude that ligand **L1** is an outstanding choice for achieving high enantioselectivity. Further screening of Cu(I) salts revealed that slightly higher C-4 regioselectivity and enantioselectivity are obtained when using copper(I) thiophene-2-carboxylate (CuTc) as the

Scheme 2. Scope of Grignard Reagents and Substrates

Scope of Grignard reagents<sup>a,b</sup>Scope of quinolines in addition reaction with  $\text{EtMgBr}$ <sup>a,b</sup>

<sup>a</sup>Only C-4-addition products are formed. The isolated yields of C-4-addition products are shown. The absolute configuration of **5b** was determined by single-crystal X-ray crystallography, and the relative configuration of **5q** was determined by NOE experiments. The absolute configurations of other compounds were assigned by analogy (for details, see the [Supporting Information](#)). <sup>b</sup>Reaction conditions: 0.1 M **1** in  $\text{CH}_2\text{Cl}_2$ , CuTc (5 mol %), L1 (6 mol %),  $\text{BF}_3 \cdot \text{Et}_2\text{O}$  (1.2–3 equiv),  $\text{RMgBr}$  (2–3 equiv) at  $-78^\circ\text{C}$  for 2–16 h (depending on the substrate and the Grignard), and then  $\text{BH}_3 \cdot \text{THF}$  (5 equiv) at  $-78^\circ\text{C}$  for 16 h. <sup>c</sup>In this case 10 mol % of L1 and 12 mol % of CuTc were used. <sup>d</sup>In this case the regioselectivity C-2/C-4 is 1/5. <sup>e</sup>In this case 15% conversion toward the C-2-addition product was observed.



copper source instead of  $\text{CuBr}\cdot\text{SMe}_2$  (Table 1, entry 8). Adopting ligand **L1** in combination with  $\text{CuTc}$  as the optimal catalyst, we continued with screening of LAs. While  $\text{Me}_3\text{SiOTf}$  activates quinoline toward both the C-2 and C-4 attacks, we hypothesized that increasing the steric bulk of the LA might reduce the background C-2 attack and direct  $\text{EtMgBr}$  toward C-4 addition. Testing several silyl-based LAs, all with  $\text{TfO}^-$  as the counterion but with different degrees of steric hindrance (Table 1, entries 9–12), we observed that the catalytic system is very sensitive to this feature of the LA. When bulky LAs are used, the C-4 attack is the main reaction pathway, albeit at the cost of dramatically decreased reactivity and enantioselectivity. At this point we decided to switch from silicon-based LAs to the slightly less reactive boron-based LA  $\text{BF}_3\cdot\text{Et}_2\text{O}$ , hoping that the diminished activation of the quinoline ring toward nucleophilic attack would allow the  $\text{Cu(I)}$  catalyst to outcompete the noncatalytic C-2 attack. Using  $\text{BF}_3\cdot\text{Et}_2\text{O}$  as the LA in the reaction without a copper catalyst (Table 1, entry 13), only 20% of the quinoline was converted to the mixture of C-2- (major product) and C-4-addition products, with 80% of the substrate remaining. Much to our delight, when combining  $\text{BF}_3\cdot\text{Et}_2\text{O}$  with the **L1**/ $\text{Cu(I)}$  complex, the reaction proceeded with absolute C-4 regioselectivity, providing the corresponding product **3a** with 58% isolated yield and more than 99% ee (Table 1, entry 14).

When  $\text{BF}_3\cdot\text{Et}_2\text{O}$  was used together with **L4**/ $\text{Cu(I)}$ , excellent regioselectivity was obtained as well, with 88% ee, but much lower conversion (Table 1, entry 15). Settling on  $\text{BF}_3\cdot\text{Et}_2\text{O}$  and **L1**/ $\text{Cu(I)}$  as the best LA and catalyst system we turned to the screening of various solvents (Table 1, entries 16–20). Remarkably, except for THF, all the solvents tested, including 2-methyltetrahydrofuran (2-Me-THF), *t*-BuOMe, toluene, and  $\text{Et}_2\text{O}$ , afforded absolute regioselectivity toward the desired addition product **3a** with almost full conversion and over 99% ee. However, the NMR yields are lower than with  $\text{CH}_2\text{Cl}_2$  (see the Supporting Information), which is therefore the solvent of choice.

Having established the optimal reaction conditions for this dearomatization protocol, we addressed the problems associated with the isolated yields of the addition product **3a**. Because of the instability of the addition product, only 58% isolated yield of **3a** with a complex mixture of byproducts was obtained, despite achieving nearly full conversion of the substrate (Table 1, entry 14). Continued attempts to optimize the reaction to eliminate the byproducts did not lead to an improved isolated yield of **3a**. Thus, we decided to change the isolation strategy and instead of trapping the addition product with acetyl chloride we attempted to reduce the addition intermediate with  $\text{BH}_3\cdot\text{THF}$  to form the tetrahydroquinoline **4a** (Scheme 2).

This strategy worked well at  $-78^\circ\text{C}$ , avoiding the formation of byproducts and providing an 83% isolated yield, thus establishing this final optimized strategy:  $\text{BF}_3\cdot\text{Et}_2\text{O}$  is used as LA in the presence of 6 mol % of chiral ligand **L1** and 5 mol % of  $\text{CuTc}$ , with  $\text{CH}_2\text{Cl}_2$  as solvent at  $-78^\circ\text{C}$ , and after addition of Grignard reagents,  $\text{BH}_3\cdot\text{THF}$  is used to reduce the dearomatized intermediate.

With the optimized conditions in hand, we started to explore the scope of this transformation, first concentrating on the addition of various types of Grignard reagents (Scheme 2). We were delighted to find that, when quinoline **1a** is used as the substrate, excellent results are obtained with both linear and sterically demanding  $\alpha$ -,  $\beta$ -, and  $\gamma$ -branched Grignard reagents

(**4a–4e**). Grignard reagents containing a terminal phenyl, a terminal double bond, or a silyl functional group are also well-tolerated, providing the corresponding products **4f**, **4g**, and **4h** with high yields and over 99% ee. It is remarkable that, except for the C-4 product obtained with *i*-PrMgBr (80% enantiomeric excess), the addition of all the tested Grignard reagents to **1a** led exclusively to the C-4-addition products with over 99% ee, proving that our catalytic system has excellent control over the reactivity as well as the regio- and enantioselectivity. Subsequently, we explored the scope of the substrates, focusing on investigating the effect of different substitutions on the quinoline upon addition with  $\text{EtMgBr}$ .

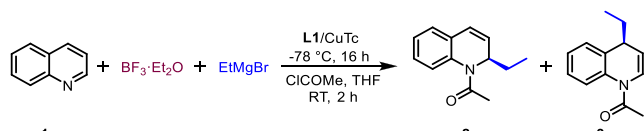
Evaluating the effect of substituents at the C-6 position, we found that addition to substrates bearing either an electron-withdrawing group (fluoro and bromo) or an electron-donating group (methyl and methoxy) leads to the corresponding C-4-addition products **5a–5d** with excellent results. The ester and cyano functional groups at the C-6 position are also tolerated, generating products **5e** and **5f** with excellent yields and ee, indicating that this catalytic system can efficiently control the regioselectivity to avoid C-2 addition as well as chemoselectivity to avoid addition to the functional groups. C-4-addition products **5g–5j**, derived from the addition of  $\text{EtMgBr}$  to substrates bearing bromo-, methyl-, methoxy-, and vinyl-substituents at the C-7 position, respectively, were obtained with high yields and enantiopurities over 99%.

Our catalytic system can even tolerate the presence of substituents at the sterically demanding 5- and 8-positions, providing the corresponding addition products **5k–5n** with high yields and excellent ee. Also, an example of a 6,7-disubstituted quinoline, bearing a conjugated phenyl ring, was successfully subjected to our catalytic system, leading to the formation of 1,4-addition product **5o** with excellent regio- and enantioselectivity. Significantly, quinolines bearing substituents at the C-2 position are also excellent substrates for this reaction, allowing access to tetrahydroquinolines **5p** and **5q** with multiple stereocenters with 6:1 diastereoselectivity and high enantiomeric excess. Contrary to these findings, no conversion was observed with C-3- and C-4-substituted quinolines. This kind of sensitivity to the substituents aligns with our observations in copper-catalyzed additions to  $\alpha,\beta$ -unsaturated amides and carboxylic acids, where it was shown that additional substitutions in the  $\alpha$ - or  $\beta$ -positions with respect to the electron-withdrawing group diminishes the reactivity of the substrates drastically and prevents copper catalysis from operating.<sup>11</sup>

It is also important to note that the reaction rate decreases with increased steric hindrance of either the substrate or the Grignard reagent, as well as with enhanced electron density of the substrate. For these reasons, increased amounts of Grignard reagent and  $\text{BF}_3\cdot\text{Et}_2\text{O}$  (3 equiv each) are required to reach full conversion toward products **4b**, **4d–4h**, **5d**, **5i**, **5l**, **5n**, **5o**, and **5q**. When using an aryl Grignard reagent, namely,  $\text{PhMgBr}$ , no conversion to the addition product was observed, even in the presence of a large excess of the corresponding Grignard reagent and  $\text{BF}_3\cdot\text{Et}_2\text{O}$ . Conversely, for substrate **5e**, the amount of LA had to be reduced from 2 to 1.2 equiv to avoid possible binding to the ester group and thus to ensure that the addition occurs selectively at the quinoline ring. For substrate **5j**, the amount of LA was also reduced to 1.2 equiv in order to reduce the formation of byproducts.

To showcase the efficacy of our catalytic protocol, we determined the reaction time needed to achieve full conversion of the substrate and studied the effect of the catalyst loading on the reaction outcome. These studies were performed on the model reaction of addition of EtMgBr to quinoline **1a** in the presence of the catalyst **L1**/Cu(I) and  $\text{BF}_3 \cdot \text{Et}_2\text{O}$ , followed by trapping with acetyl chloride (Table 2).

**Table 2. Effect of the Catalyst Loading on the Reaction Outcome<sup>a</sup>**



entry	<b>L1</b> /Cu(I) [mol %]	<b>1a</b> : <b>2a</b> : <b>3a</b> <sup>b</sup>	ee ( <b>3a</b> ) [%] <sup>c</sup>
1	5	1:0:99	>99
2 <sup>d</sup>	5	6:0:94	>99
3	1	5:0:95	>99
4	0.1	5:0:95	99
5	0.01	58:19:23	40

<sup>a</sup>Reaction conditions: 0.1 M **1a** in  $\text{CH}_2\text{Cl}_2$ ,  $\text{BF}_3 \cdot \text{Et}_2\text{O}$  (2 equiv), EtMgBr (2 equiv) at  $-78^\circ\text{C}$  for 16 h, and then THF (4 mL), ClCOMe (5 equiv) at RT for 2 h. <sup>b</sup>The ratio was determined by  $^1\text{H}$  NMR of reaction crude. <sup>c</sup>Enantiomeric excess was determined by HPLC on a chiral stationary phase. <sup>d</sup>The reaction time of addition step is 10 min.

First, we tested the reaction with 5 mol % of catalyst loading for a reaction time of 10 min and found that product **3a** was obtained with 94% conversion and over 99% ee (Table 2, entry 2). We were also pleasantly surprised by the fact that reducing the catalyst loading from 5 to 1 mol %, and even further to 0.1 mol %, did not affect the reaction outcome, still promoting the conversion of the substrate to the C-4-addition product with nearly full conversion and 99% enantiopurity (Table 2, entries 3 and 4). These results are remarkable when compared to other catalytic enantioselective methods using Grignard reagents: a TON of 1000 represents the highest TON among all the catalytic asymmetric reactions performed with Grignard reagents reported today. We also tested the scaling up of our catalytic system by performing the addition reaction of EtMgBr to 1.3 g of quinoline **1a** (a 20-fold scale-up) with 0.1 mol % of **L1**/Cu(I), followed by reduction with  $\text{BH}_3 \cdot \text{THF}$ . The corresponding product **4a**, which is a key intermediate for the synthesis of drug candidate (S)-LG121071, a selective androgen receptor modulator (SARM),<sup>12</sup> was obtained with 71% yield and 96% ee (Scheme 3).

The mechanism of this transformation might follow a pathway analogous to the one proposed for the copper-catalyzed addition of organocuprates to  $\alpha,\beta$ -unsaturated

carbonyl compounds.<sup>13</sup> However, since in our system the  $\alpha,\beta$ -unsaturated imine moiety is part of an aromatic ring, a LA and a copper complex (**L1**/Cu) are needed to activate the substrate and overcome the high energy barrier induced by the dearomatization during the addition reaction. The number of reagents involved, and the fact that this allows complete enantio- and regiocontrol, implies a complex mechanistic picture in which subtle details control the reaction outcome. To gain insight into the reaction mechanism and specifically the role of LA and the **L1**/Cu(I) catalyst system on the reactivity and selectivity (regio- and stereoselectivities) we have carried out thorough molecular modeling studies (Figures 1 and 2). For the modeling we adopted the quinoline (**1a**)/ $\text{BF}_3$ /**L1**–CuBr/EtMgBr reaction system.

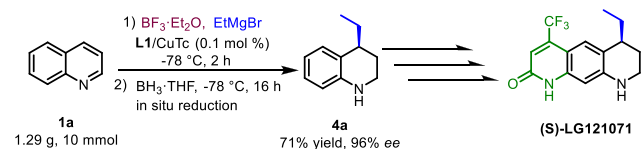
Upon addition of  $\text{BF}_3$  to quinoline **1a** a new complex **1a**– $\text{BF}_3$  is formed in a highly exergonic process ( $\Delta G = -20.3$  kcal/mol). This complexation induces a change of charges at carbons C-2 and C-4 from 0.33 and 0.24 au in **1a** to 0.44 and 0.43 au in **1a**– $\text{BF}_3$ , confirming significant activation of quinoline toward nucleophilic additions but also explaining why the addition of Grignard reagent to **1a**– $\text{BF}_3$  in the absence of copper complex catalyst is not regioselective: the charges on both carbons are rather similar (see Figure 1a and Table 1, entry 13).

A systematic density functional theory (DFT) analysis on the relative stability of the copper species that might be present in the reaction media revealed that, once the copper source and **L1** can interact, they will form the complex **L1**–CuBr ( $\Delta G = -20.91$  kcal/mol). At the same time, the large excess of Grignard reagent wrt **L1**–CuBr leads us to propose that direct transmetalation of **L1**–CuBr will afford the organocopper species **I**, which is thermodynamically preferred ( $-32.70$  kcal/mol) and also the starting point for the catalytic cycle (see Figure 1a and the Supporting Information). Having identified the active forms of the substrate (**1a**– $\text{BF}_3$ ) and the catalyst (**I**), we explored their interaction: species **I** can approach the LA-activated substrate **1a**– $\text{BF}_3$  to form either of species **II** depending on the regioselectivity (C-2 vs C-4) of the reaction. Once species **II** has been formed, it evolves further via the transfer of the Et group from the copper center to either the C-2 or C-4 position of quinoline to form the respective species **III**. This step is followed by the addition of the second molecule of EtMgBr to the copper center of species **III**, thus promoting the release of either C-4- or C-2-addition product intermediate **IV** and the recovery of the organocopper species **I**. Our modeling studies described below provide full rationalization for the experimentally observed C-4 selectivity and the stereochemistry of the process.

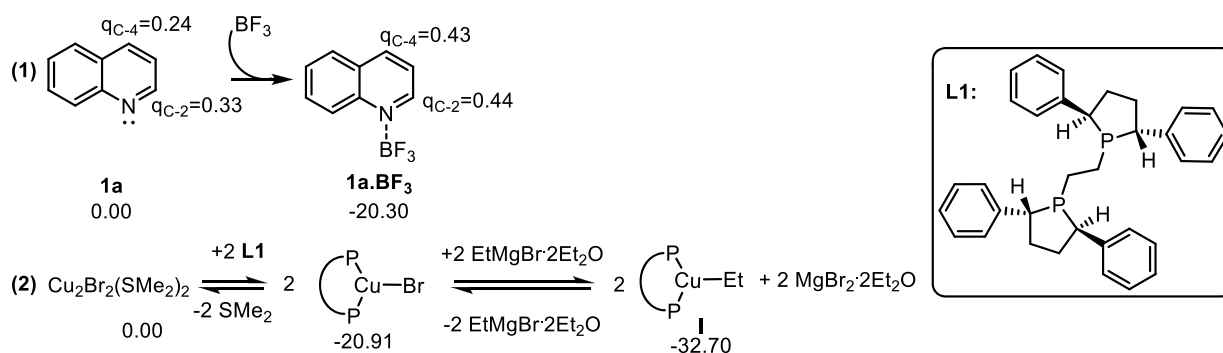
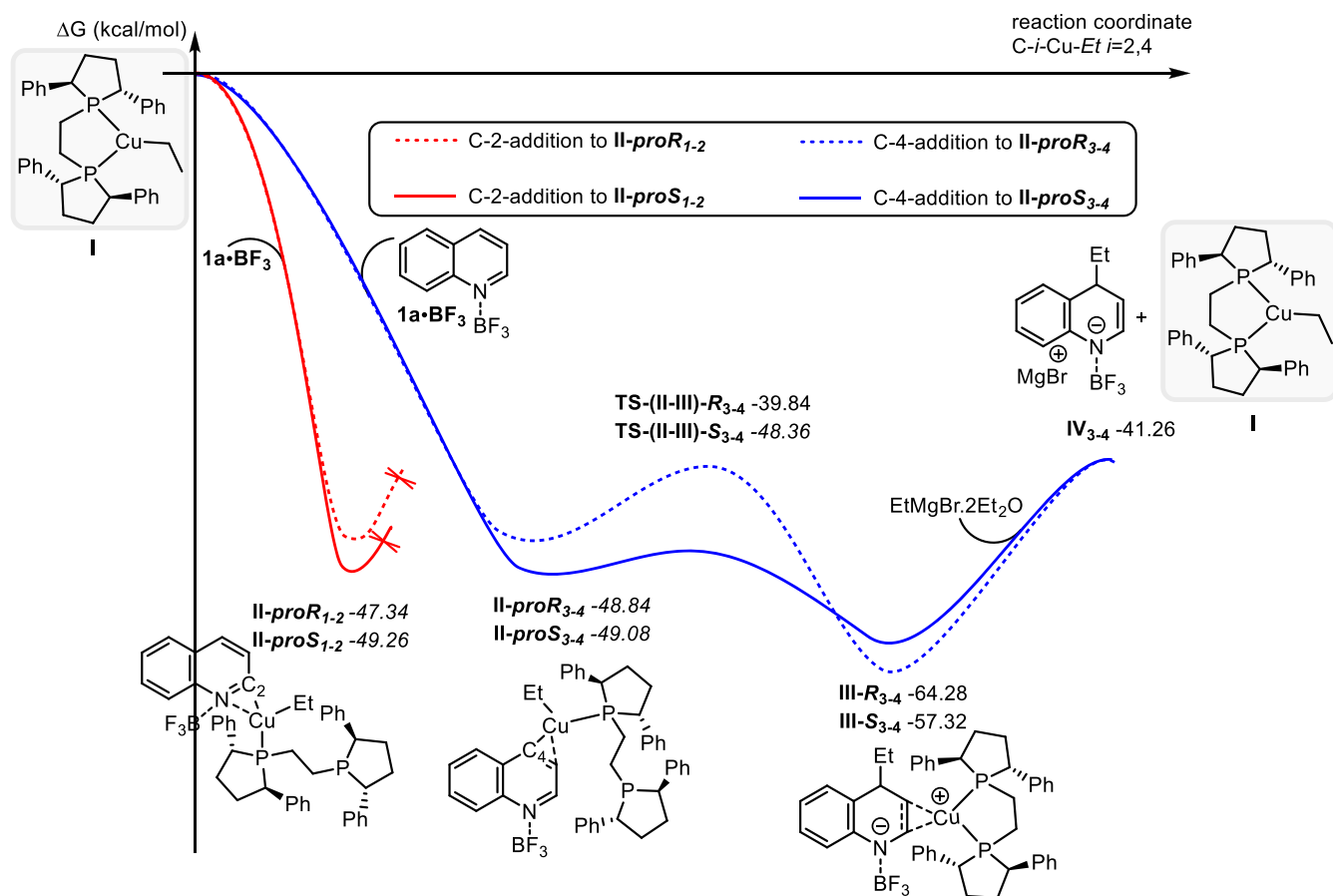
In the first step of the catalytic cycle species **I** can, *a priori*, bind to either of the two faces of **1a**– $\text{BF}_3$  and either to the N–C-2 or the C-3–C-4 region, thus leading to two sets of possible diastereomeric complexes (**II**–*proR*<sub>1–2</sub>, **II**–*proS*<sub>1–2</sub>, **II**–*proR*<sub>3–4</sub>, **II**–*proS*<sub>3–4</sub>), all of which are thermodynamically favorable and very close in energy (from  $-47.34$  to  $-49.26$  kcal/mol); see Figure 1b.

A detailed structural analysis of these four complexes reveals that the dangling uncoordinated branch in the ligand in species **II**<sub>3–4</sub> is oriented toward the outside of the molecule, preventing destabilizing steric interactions with the substrate while also inhibiting a differentiation between both diastereomers. Alternatively, in species **II**<sub>1–2</sub> the ligand is located on top of the molecule (toward the LA) but too far from the quinoline for an energetic differentiation (Figure 2). Interestingly, we

**Scheme 3. Twenty-Fold Scale-Up Synthesis of Product **4a**, a Key Intermediate for Preparation of Drug Candidate (S)-LG121071**



## (a) Identification of the active catalyst (1) and substrate (2)

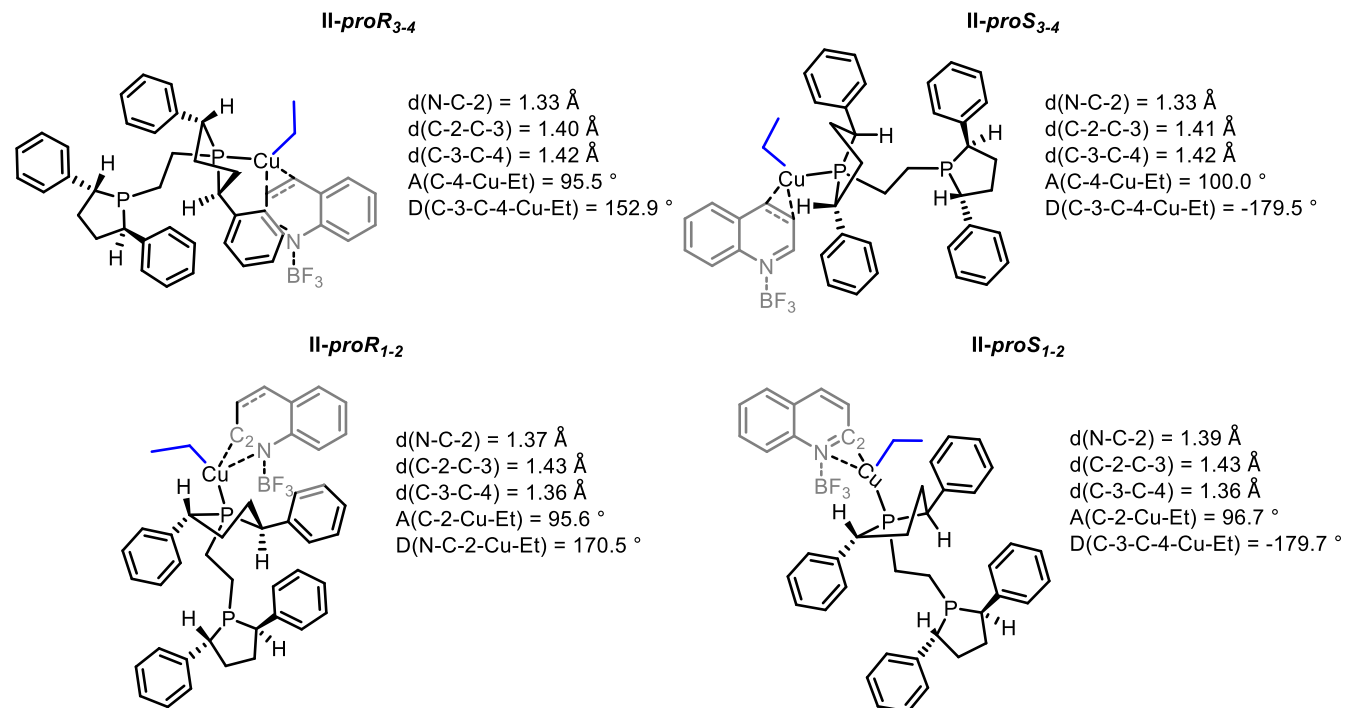
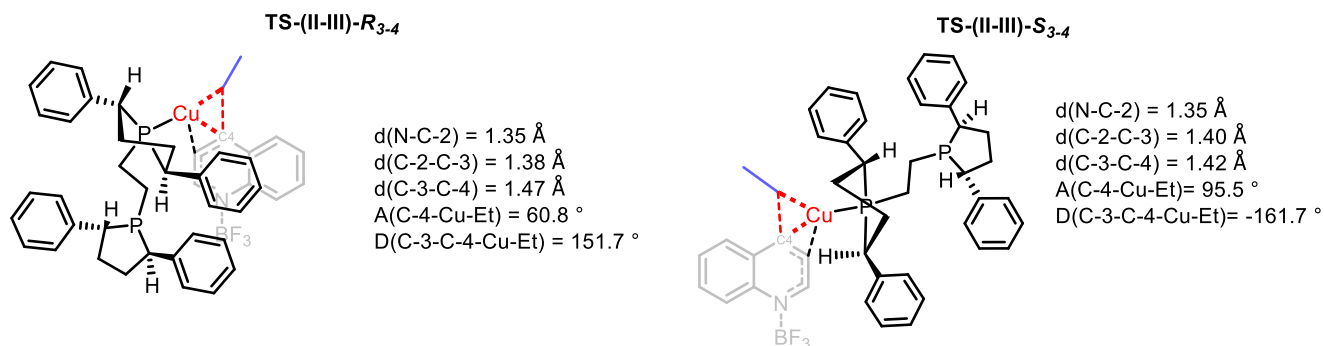
(b) Energy profile (2) of the C-4- vs C-2-addition of  $L1CuEt$  (I) to  $1a \cdot BF_3$ 

**Figure 1.** DFT mechanistic studies for the copper-catalyzed asymmetric C-4 addition of  $EtMgBr$  to quinoline. (a) Identification of the active forms of the quinoline (1) and the catalyst (2) in the reaction media. The ligand **L1** is represented by an arc at the proposed equilibria for simplicity. (b) Energy profile for the copper-catalyzed asymmetric C-2 and C-4 addition of  $EtMgBr$  to  $1a \cdot BF_3$ . Calculations were performed at the PCM<sup>14</sup> ( $CH_2Cl_2$ )/M06<sup>15</sup>/def2svp<sup>16</sup> computational level using the Gaussian 09 program.<sup>17</sup> The thermochemistry was obtained at 1 atm and 195 K. Red lines mark the C-2-addition path, while blue lines indicate the C-4-addition path. The depicted charges correspond to APT charges with hydrogens summed into heavy atoms. The reported relative energies are computed wrt  $1a/BF_3/2xEtMgBr-2Et_2O/I$  and expressed in kcal/mol.

found that, in order for the complexes **II** to be formed, one of the hemilabile phosphorus atoms of the ligand has to abandon the first-coordination sphere of the copper center so that a new coordination vacancy is created and the quinoline molecule can be accommodated. Once the complex **II** is formed, the evolution of the resulting diastereomeric pairs via the transfer of the Et group from the copper center to either the C-2 or C-4 position of quinoline to form species **III** differs in terms of energy.

Turning first to the C-4 pathway with species **II**<sub>3-4</sub>: the evolution of  $II-proR_{3-4}$  involves an energy barrier of 9.0 kcal/mol, while the analogous evolution of  $II-proS_{3-4}$  is only 0.7 kcal/mol. Thus, the formation of species **III** constitutes the enantiodetermining step. The difference in energy between the two diastereoisomers can be rationalized by analyzing the transition state structures  $TS-(II-III)-R_{3-4}$  and  $TS-(II-III)-S_{3-4}$ . The delivery of the ethyl group in  $TS-(II-III)_{3-4}$  requires a decrease of the C-4-Cu-Et angle due to the

## (a) Structural analysis of intermediates II

(b) Structural analysis of the transition states TS-(II-III)<sub>3-4</sub>

**Figure 2.** Structural analysis and 3D representation of relevant intermediates. (a) Intermediates II. (b) Transition states TS-(II-III)<sub>3-4</sub>. The copper center and the bonds participating in the reaction coordinate (decreasing of C-4-Cu-Et angle) are marked in red. For visualization purposes we have depicted the ligand in black, the substrate in gray (the substrate is always oriented in the plane of the paper), and the ethyl group being transferred in blue. The letters “d”, “A”, and “D” are used to indicate bond distances in angstroms (Å) and angles and dihedral angles in degrees (deg), respectively.

approach of the ligand moiety to the quinoline part. In the case of TS-(II-III)-*R*<sub>3-4</sub>, a phenyl group in the ligand moiety is pointing to the quinoline; thus, the decrease of the C-4-Cu-Et angle results in a slight energy penalization due to the clash between the phenyl group and the quinoline in the transition state. In the TS-(II-III)-*S*<sub>3-4</sub> the phenyl group is pointing away from the quinoline, and thus the resulting lower steric hindrance makes this transition state energetically much more favorable. On the other hand, our attempts to localize the transition states for the C-2-addition case (from II<sub>1-2</sub> to III<sub>1-2</sub>) resulted surprisingly in the release of organocopper species I from II<sub>1-2</sub>.

Intrigued by these results we studied the evolution of the energy of II-*proR*<sub>1-2</sub> with the variation of the reaction coordinate (decrease of the C-2-Cu-Et angle) and found that this movement entails the separation of the copper from

the quinoline and results in a weak complex between I and 1a-BF<sub>3</sub>. In this complex the copper is already located in the C-3-C-4 region, thus predisposing the system to evolve via the C-4 addition. The main difference between the evolution of II<sub>3-4</sub> via C-4 addition and II<sub>1-2</sub> via C-2 addition resides in the ability of the environment to stabilize the transient structures during the reorganization of copper(I) species while the ethyl group moves from the copper center to the C-2 or C-4 position. In the case of the C-4 addition the decrease of the C-4-Cu-Et angle is accompanied by an incipient stabilizing interaction of the copper with the C-2-C-3 bond, whereas this interaction is not possible when the C-2-Cu-Et angle is decreased. On the contrary, the LA prevents the copper center from interacting with the nitrogen for possible stabilization, thus resulting in the release of the organocopper species I (for details see the Supporting Information).



Thus, our molecular modeling has shown that the regio- and the enantioselectivity in this reaction are determined in the second step of the proposed catalytic cycle and that the complex **II** is predisposed to evolve via C-4 addition. The results also reveal that the role of the LA is not only to activate the substrate **1a** toward a potential nucleophilic addition but also to subtly control the regiochemistry by preventing the C-2 addition from happening. These findings are in line with the tolerance of the reaction to quinoline substituents at the C-2 position and the sensitivity to a substituent in the C-3 and C-4 positions.

## CONCLUSIONS

We have presented the first copper-catalyzed enantioselective strategy for the dearomatization of nitrogen-containing heteroaromatics in the presence of Lewis acid. We have shown that the synergistic action of Lewis acid, chiral copper catalyst, and Grignard reagents provides direct access to the chiral dearomatized products with excellent regioselectivity and enantioselectivity and with a catalyst TON as high as 1000. Furthermore, we were able to unravel the roles of both the Lewis acid and the copper complex and prove that the former is responsible not only for the activation of the substrate but also for the control of the regioselectivity and the latter for controlling the enantioselectivity and further activating the substrate. Our results together with modeling studies support mechanistic connection between copper-catalyzed conjugate additions of organometallics to non-aromatic carbonyl-based Michael acceptors on the one hand and to aromatic quinolines on the other.

## ASSOCIATED CONTENT

### Supporting Information

The Supporting Information is available free of charge at <https://pubs.acs.org/doi/10.1021/jacs.0c09974>.

Experimental procedures and characterization data, X-ray structure determination, computational details, and NMR spectra (PDF)

Crystallographic data in CIF format for **5bCIF**

## AUTHOR INFORMATION

### Corresponding Author

Syuzanna R. Harutyunyan – Stratingh Institute for Chemistry, University of Groningen, 9747 AG Groningen, The Netherlands; [orcid.org/0000-0003-2411-1250](https://orcid.org/0000-0003-2411-1250); Email: [S.Harutyunyan@rug.nl](mailto:S.Harutyunyan@rug.nl)

### Authors

Xingchen Yan – Stratingh Institute for Chemistry, University of Groningen, 9747 AG Groningen, The Netherlands

Luo Ge – Stratingh Institute for Chemistry, University of Groningen, 9747 AG Groningen, The Netherlands

Marta Castiñeira Reis – Stratingh Institute for Chemistry, University of Groningen, 9747 AG Groningen, The Netherlands

Complete contact information is available at: <https://pubs.acs.org/doi/10.1021/jacs.0c09974>

### Author Contributions

<sup>†</sup>X.Y. and L.G. contributed equally to this work.

### Notes

The authors declare no competing financial interest.

## ACKNOWLEDGMENTS

Financial support from the European Research Council (S.R.H. Grant No. 773264, LACOPAROM), the China Scholarship Council (CSC, to X.Y. and L.G.), and the Ministry of Education, Culture and Science (Gravity program 024.001.035 to S.R.H.) is acknowledged. M.C.R. thanks the Centro de Supercomputación de Galicia (CESGA) for the free allocation of computational resources and the Xunta de Galicia (Galicia, Spain) for financial support through the ED481B-Axudas de apoio á etapa de formación posdoutoral (modalidade A) fellowship. This work was partially carried out on the Dutch national e-infrastructure with the support of SURF Cooperative.

## REFERENCES

- (1) (a) Pozharskii, A. F.; Soldatenkov, A.; Katritzky, A. R. *Heterocycles in Life and Society: An Introduction to Heterocyclic Chemistry, Biochemistry and Applications*, 2nd ed.; Wiley: Chichester, U.K., 2011. (b) Blacker, J. A.; Williams, M. T. *Pharmaceutical Process Development: Current Chemical and Engineering Challenges*; Royal Society of Chemistry: Cambridge, U.K., 2011.
- (2) (a) Mitchenson, A.; Nadin, A. Saturated nitrogen heterocycles. *J. Chem. Soc., Perkin Trans.* **2000**, 1, 2862–2892. (b) Muthukrishnan, I.; Sridharan, V.; Menéndez, J. C. Progress in the Chemistry of Tetrahydroquinolines. *Chem. Rev.* **2019**, 119, 5057–5191. (c) Sridharan, V.; Suryavanshi, P. A.; Menendez, J. C. Advances in the chemistry of tetrahydroquinolines. *Chem. Rev.* **2011**, 111, 7157–7259. (d) Katritzky, A. R.; Rachwal, S.; Rachwal, B. Recent progress in the synthesis of 1,2,3,4-tetrahydroquinolines. *Tetrahedron* **1996**, 52, 15031–15070.
- (3) (a) Lovering, F.; Bikker, J.; Humblet, C. Escape from flatland: increasing saturation as an approach to improving clinical success. *J. Med. Chem.* **2009**, 52, 6752–6756. (b) Clemons, P. A.; Bodycombe, N. E.; Carrinski, H. A.; Wilson, J. A.; Shamji, A. F.; Wagner, B. K.; Koehler, A. N.; Schreiber, S. L. Small molecules of different origins have distinct distributions of structural complexity that correlate with protein-binding profiles. *Proc. Natl. Acad. Sci. U. S. A.* **2010**, 107, 18787–18792.
- (4) (a) You, S.-L. *Asymmetric Dearomatization Reactions*; Wiley-VCH: Weinheim, Germany, 2016. (b) López Ortiz, F. L.; Iglesias, M. J.; Fernández, I.; Andújar Sánchez, C. M. A.; Ruiz Gómez, G. R. Nucleophilic Dearomatizing (DNAr) Reactions of Aromatic C<sub>6</sub>H<sub>5</sub> Systems. *Chem. Rev.* **2007**, 107, 1580–1691. (c) Zhuo, C.; Zhang, W.; You, S.-L. Catalytic asymmetric dearomatization reactions. *Angew. Chem., Int. Ed.* **2012**, 51, 12662–12686.
- (5) Jones, G. *The Chemistry of Heterocyclic Compounds*; Wiley: Bristol, U.K., 1982.
- (6) (a) Takamura, M.; Funabashi, K.; Kanai, M.; Shibasaki, M. Asymmetric Reissert-type reaction promoted by bifunctional catalyst. *J. Am. Chem. Soc.* **2000**, 122, 6327–6328. (b) Takamura, M.; Funabashi, K.; Kanai, M.; Shibasaki, M. Catalytic enantioselective Reissert-Type reaction: development and application to the synthesis of a potent NMDA receptor antagonist (–)-L-689,560 using a solid-supported catalyst. *J. Am. Chem. Soc.* **2001**, 123, 6801–6808. (c) Pappoppula, M.; Cardoso, F. S. P.; Garrett, B. O.; Aponick, A. Enantioselective copper-catalyzed quinoline alkylation. *Angew. Chem.* **2015**, 127, 15417–15421. (d) Wang, Y.; Liu, Y.; Zhang, D.; Wei, H.; Shi, M.; Wang, F. Enantioselective rhodium-catalyzed dearomative arylation or alkenylation of quinolinium salts. *Angew. Chem., Int. Ed.* **2016**, 55, 3776–3780. (e) Yamaoka, Y.; Miyabe, H.; Takemoto, Y. Catalytic enantioselective Petasis-type reaction of quinolines catalyzed by a newly designed thiourea catalyst. *J. Am. Chem. Soc.* **2007**, 129, 6686–6687. (f) Zurro, M.; Asmus, S.; Beckendorf, S.; Mück-Lichtenfeld, C.; Mancheño, O. G. Chiral helical oligotriazoles: new class of anion-binding catalysts for the asymmetric dearomatization of electron-deficient N-heteroarenes. *J. Am. Chem. Soc.* **2014**, 136, 13999–14002. (g) Fischer, T.; Duong, Q.-N.; García

Mancheño, O. G. Triazole-based anion-binding catalysis for the enantioselective dearomatization of N-heteroarenes with phosphorus nucleophiles. *Chem. - Eur. J.* **2017**, *23*, 5983–5987. (h) Cointeaux, L.; Alexakis, A. Enantioselective addition of organolithium reagents to quinoline catalyzed by 1,2-diamines. *Tetrahedron: Asymmetry* **2005**, *16*, 925–929.

(7) Amiot, F.; Cointeaux, L.; Jan Silve, E. J.; Alexakis, A. Enantioselective nucleophilic addition of organometallic reagents to quinoline: regio-, stereo- and enantioselectivity. *Tetrahedron* **2004**, *60*, 8221–8231.

(8) (a) Meyers, A. I.; Wettlaufer, D. G. Complete intramolecular transfer of a central chiral element to an axial chiral element. Oxidation of (S)-4-naphthyl-dihydroquinolines to (S)-4-naphthyl-quinolines. *J. Am. Chem. Soc.* **1984**, *106*, 1135–1136. (b) Mohiti, M.; Rampalakos, C.; Feeney, K.; Leonori, D.; Aggarwal, V. K. Asymmetric addition of chiral boron-ate complexes to cyclic iminium ions. *Chem. Sci.* **2014**, *5*, 602–607.

(9) Mani, N. S.; Chen, P.; Jones, T. K. Addition of Grignard reagents to quinolinium salts: evidence for a unique redox reaction between a 1,4- and a 1,2-dihydroquinoline. *J. Org. Chem.* **1999**, *64*, 6911–6914.

(10) (a) Perlmutter, P. *Conjugate Addition Reactions in Organic Synthesis*; Tetrahedron Organic Chemistry, Vol. 9; Pergamon: Oxford, U.K., 1992. (b) Harutyunyan, S. R.; den Hartog, T.; Geurts, K.; Minnaard, A. J.; Feringa, B. L. Catalytic asymmetric conjugate addition and allylic alkylation with Grignard reagents. *Chem. Rev.* **2008**, *108*, 2824–2852. (c) Alexakis, A.; Krause, N.; Woodward, S. *Copper-Catalyzed Asymmetric Synthesis*; Wiley-VCH: Weinheim, Germany, 2014. (d) Howell, G. P. Asymmetric and diastereoselective conjugate addition reactions: C–C bond formation at large scale. *Org. Process Res. Dev.* **2012**, *16*, 1258–1272.

(11) (a) Jumde, R. P.; Lanza, F.; Veenstra, M. J.; Harutyunyan, S. R. Catalytic asymmetric addition of Grignard reagents to alkenyl-substituted aromatic N-heterocycles. *Science* **2016**, *352*, 433–437. (b) Rodríguez-Fernández, M.; Yan, X.; Collados, J. F.; White, P. B.; Harutyunyan, S. R. Lewis acid enabled copper-catalyzed asymmetric synthesis of chiral  $\beta$ -substituted amides. *J. Am. Chem. Soc.* **2017**, *139*, 14224–14231. (c) Rong, J.; Oost, R.; Desmarchelier, A.; Minnaard, A. J.; Harutyunyan, S. R. Catalytic asymmetric alkylation of acylsilanes. *Angew. Chem., Int. Ed.* **2015**, *54*, 3038–3042. (d) Yan, X.; Harutyunyan, S. R. Catalytic enantioselective addition of organometallics to unprotected carboxylic acids. *Nat. Commun.* **2019**, *10*, 3402.

(12) Hamann, L. G.; Mani, N. S.; Davis, R. L.; Wang, X.-N.; Marschke, K. B.; Jones, T. K. Discovery of a potent, orally active, nonsteroidal androgen receptor agonist: 4-ethyl-1,2,3,4-tetrahydro-6-(trifluoromethyl)-8-pyridono[5,6-g]-quinoline (LG121071). *J. Med. Chem.* **1999**, *42*, 210–212.

(13) (a) Yoshikai, N.; Nakamura, E. Mechanisms of nucleophilic organocopper (I) reactions. *Chem. Rev.* **2012**, *112*, 2339–2372. (b) Yamanaka, M.; Inagaki, A.; Nakamura, E. Theoretical studies on structures and reactivities of organocuprate (I) and organocopper (III) species. *J. Comput. Chem.* **2003**, *24*, 1401–1409. (c) Harutyunyan, S. R.; Lopez, F.; Browne, W. R.; Correa, A.; Peña, D.; Badorrey, R.; Meetsma, A.; Minnaard, A. J.; Feringa, B. L. On the mechanism of the copper-catalyzed enantioselective 1,4-addition of Grignard reagents to  $\alpha,\beta$ -unsaturated carbonyl compounds. *J. Am. Chem. Soc.* **2006**, *128*, 9103–9118.

(14) Tomasi, J.; Mennucci, B.; Cammi, R. Quantum mechanical continuum solvation models. *Chem. Rev.* **2005**, *105*, 2999–3093.

(15) Zhao, Y.; Truhlar, D. G. The M06 suite of density functionals for main group thermochemistry, thermochemical kinetics, non-covalent interactions, excited states, and transition elements: Two new functionals and systematic testing of four M06-class functionals and 12 other functionals. *Theor. Chem. Acc.* **2008**, *120*, 215–241.

(16) Weigend, F.; Ahlrichs, R. Balanced basis sets of split valence, triple zeta valence and quadruple zeta valence quality for H to Rn: Design and assessment of accuracy. *Phys. Chem. Chem. Phys.* **2005**, *7*, 3297–3305.

(17) Frisch, M. J.; Trucks, G. W.; Schlegel, H. B.; Scuseria, G. E.; Robb, M. A.; Cheeseman, J. R.; Scalmani, G.; Barone, V.; Mennucci, B.; Petersson, G. A.; Nakatsuji, H.; Caricato, M.; Li, X.; Hratchian, H. P.; Izmaylov, A. F.; Bloino, J.; Zheng, G.; Sonnenberg, J. L.; Hada, M.; Ehara, M.; Toyota, K.; Fukuda, R.; Hasegawa, J.; Ishida, M.; Nakajima, T.; Honda, Y.; Kitao, O.; Nakai, H.; Vreven, T.; Montgomery, J. A., Jr.; Peralta, J. E.; Ogliaro, F.; Bearpark, M.; Heyd, J. J.; Brothers, E.; Kudin, K. N.; Staroverov, V. N.; Kobayashi, R.; Normand, J.; Raghavachari, K.; Rendell, A.; Burant, J. C.; Iyengar, S. S.; Tomasi, J.; Cossi, M.; Rega, N.; Millam, J. M.; Klene, M.; Knox, J. E.; Cross, J. B.; Bakken, V.; Adamo, C.; Jaramillo, J.; Gomperts, R.; Stratmann, R. E.; Yazyev, O.; Austin, A. J.; Cammi, R.; Pomelli, C.; Ochterski, J. W.; Martin, R. L.; Morokuma, K.; Zakrzewski, V. G.; Voth, G. A.; Salvador, P.; Dannenberg, J. J.; Dapprich, S.; Daniels, A. D.; Farkas, O.; Foresman, J. B.; Ortiz, J. V.; Cioslowski, J.; Fox, D. J. *Gaussian 09*, revision A.02; Gaussian, Inc.: Wallingford, CT, 2009.